

Updated evaluation metrics for optimal intensity measure selection in probabilistic seismic demand models

Farid Khosravikia*, Patricia Clayton

Dept. of Civil, Architectural and Environmental Engineering, The University of Texas at Austin, Austin, TX, United States



ARTICLE INFO

Keywords:

Optimal intensity measure
 Probabilistic seismic demand models
 Performance-based earthquake engineering
 Bridge infrastructure
 Human-induced seismicity

ABSTRACT

This study proposes an update on the criteria that are typically used to select the optimal intensity measures (IMs) for development of probabilistic seismic demand models (PSDMs), which relate the input seismic hazard and structural responses. Employing an optimal IM contributes to decreasing the uncertainty in the PSDMs, which, in turn, increases the reliability of the PSDMs used in performance-based earthquake engineering analyses. In the literature, the optimality of the IMs is generally evaluated by the following metrics: efficiency; practicality; proficiency, which is the composite of efficiency and practicality; sufficiency; and hazard computability. The present study shows that the current criteria for evaluating the practicality and proficiency features may mislead the selection of the optimal IM when IMs with different ranges and magnitudes are investigated. Moreover, the efficiency metric can provide biased results when comparing IMs for predicting demands of different structural components or types of systems. As a result, alternative solutions are proposed to investigate the efficiency, practicality, and proficiency features of the IMs. The suggested metrics are employed in a case study to evaluate the IMs used to develop PSDMs for multi-span continuous steel girder bridges in Texas subjected to human-induced seismic hazard.

1. Introduction

Current performance-based earthquake engineering frameworks [1] contain four main analysis steps: seismic hazard analysis, structural seismic response analysis, damage analysis, and loss estimation. In probabilistic frameworks, the structural response and demand are often characterized by probabilistic seismic demand models (PSDMs), which provide the relationship between the structural demand responses (e.g., component deformations, accelerations, internal forces, etc.) and the ground motion intensity measure (IM). The peak ground acceleration (PGA), peak ground velocity (PGV), and spectral acceleration at different periods ($S_a(T)$) are the most common IMs used for engineering applications. PSDMs provide the conditional probability that the structural demand (D) meets or exceeds a certain value (d) given the ground motion intensity measure ($P[D \geq d | IM]$).

The reliability of the outcomes of the probabilistic framework depends on the level of uncertainty associated with the PSDMs, which, in turn, depends on the selection of the IM for the model. Proper selection of the IM reduces the uncertainty in the PSDMs, thereby leading to more reliable performance predictions. In this regard, previous researchers proposed metrics to evaluate IM optimality, which most commonly include efficiency, practicality, proficiency, sufficiency, and

computability as described in detail in Section 3.

These metrics have been used in many studies to investigate IM optimality for different structures subjected to different seismic hazards. For example, Mackie and Stojadinovic [2] compared the optimality of fifteen different IMs for California highway bridges, and they demonstrated that spectral acceleration and displacement at the natural period are the most appropriate IMs as they reduce uncertainties in the PSDMs. Padgett et al. [3] evaluated ten different IMs for highway bridge portfolios in Central and Eastern United States, and they found that PGA is a preferred IM based on the abovementioned characteristics. More recently, Hariri-Ardebili and Saouma [4] used these criteria to examine over 70 different IMs for a concrete gravity dam. They found that among the ground motion-dependent scalar IM parameters, PGV is the most optimal IM for the concrete gravity dam. Wang et al. [5] investigated the optimality of 26 different IMs for extended pile-shaft-supported bridges in liquefiable and laterally spreading soils. They concluded that velocity-related IMs result in more reliable PSDMs for the considered system compared to acceleration, displacement, and time-related IMs.

The present study, first, shows that the current criterion for investigating efficiency can produce biased results when evaluating different components or systems that have different magnitudes of

* Corresponding author.

E-mail addresses: farid.khosravikia@utexas.edu (F. Khosravikia), clayton@utexas.edu (P. Clayton).

demand. Moreover, it is shown that the practicality metric may mislead the selection of the optimal IM when IMs with different ranges and magnitudes are investigated. This criterion may, in turn, adversely affect the proficiency feature which is often used to determine the IM considering both efficiency and practicality. Hence, alternative solutions are proposed for efficiency, practicality, and proficiency metrics of evaluation. The updated framework can be used not only for investigating the optimality of the different IMs on a single demand parameter, but also for comparing the optimality of an IM for different components of a structure or even for different systems.

The updated framework is then applied to a case study to comparatively investigate the differences in conventional and proposed metrics. The case study considered in this paper is the evaluation of multi-span continuous steel girder bridges, hereafter referred to as steel girder bridges for brevity, in the state of Texas. According to Khosravikia et al. [6], steel girder bridges are one of the main bridge types in the state of Texas, representing approximately 11% of the highway bridge inventory in the state. The motivation for the considered case study comes from the recent increase in the seismicity rate in Texas and surrounding states as a result of more intense natural gas production and petroleum activities since 2008 [7–11]. Such earthquakes generally occur in areas that historically have had negligible seismicity, where the infrastructure is designed for little to no consideration of seismic demands, thus raising concerns over the safety of infrastructure in this area. In this regard, the present study aims to find the optimal IM for probabilistic seismic demand models of the bridge infrastructure subjected to human-induced earthquakes in the considered region. This information can be used to conduct more accurate and reliable performance-based assessment of the bridge portfolios in Texas.

2. Probabilistic seismic demand models

It is conventionally assumed that conditional PSDMs follow a log-normal distribution as follows:

$$P[D \geq d | IM] = 1 - \Phi\left(\frac{\ln(d) - \ln(S_D)}{\beta_{D|IM}}\right) \quad (1)$$

where Φ is the standard normal cumulative distribution function; S_D and $\beta_{D|IM}$ are, respectively, the median value of the demand in relation to IM and the logarithmic dispersion of the demand conditioned on IM. Moreover, previous studies starting with Cornell et al. [12] showed that the median of seismic demands can be assumed to follow a power function of intensity measure as follows:

$$S_D = aIM^b \quad (2)$$

This equation can be rearranged to natural log space where $\ln(S_D)$ is a linear function with respect to $\ln(IM)$ with coefficients $\ln(a)$ and b , as follows,

$$\ln(S_D) = \ln(a) + b \times \ln(IM) \quad (3)$$

Therefore, as shown in Fig. 1, coefficients a and b can be computed by fitting a linear regression to the lognormal of the outputs (D) from nonlinear time history analyses. As seen in the figure, assuming a log-normal distribution for the conditional seismic demand results in a normal distribution with median of $\ln(S_D)$ and dispersion of $\beta_{D|IM}$ in the transformed space. According to Padgett et al. [3], $\beta_{D|IM}$ is approximately estimated by computing the dispersion of the data around the fitted linear regression using the following equation:

$$\beta_{D|IM} = \sqrt{\frac{\sum_{i=1}^N [\ln(d_i) - \ln(S_D)]^2}{N - 2}} \quad (4)$$

It is worth noting that the assumptions of using a power function (i.e. Eq. (2)) to model demand parameters with respect to IMs and

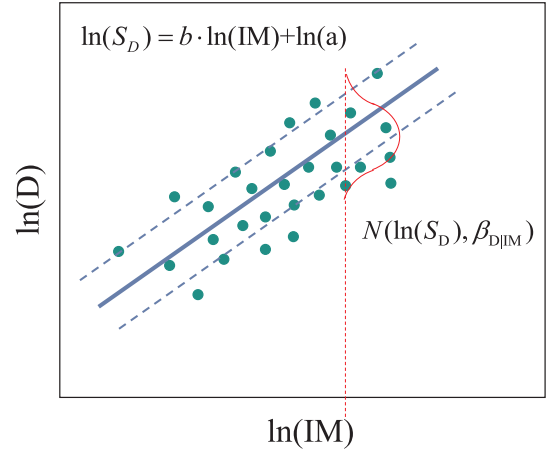


Fig. 1. Illustration of PSDMs in natural log space.

assuming a constant dispersion for the variation of a demand parameter given an IM are not the only possible models for predicting seismic responses of structures given IMs. Nonlinear models such as Artificial Neural Networks [13] can also be used to estimate the median of the demand parameters; see, for example, Lagaros and Fragiadakis [14], Mitropoulou and Papadrakakis [15], as well as Wang et al. [16], among others.

3. Conventional framework of optimal IM selection

Five different criteria have been typically used in the literature to investigate the optimality of the intensity measures as: efficiency, sufficiency [17], practicality [2], proficiency [3], and hazard computability [18]. Each of these metrics is briefly explained below.

3.1. Efficiency

The first criterion is the efficiency of the IM, which determines the variation of the predicted demand for a given IM and is quantified by parameter $\beta_{D|IM}$ shown in Eq. (4). More efficient IMs lead to lower values of $\beta_{D|IM}$, indicating less dispersion around the estimated demand from Eq. (3).

3.2. Practicality

The second criterion is practicality, which is an indicator of the dependency of the demand on the IM. For conventional linear models, this criterion is quantified by the parameter b in Eq. (3), which is the slope of the linear regression. Values close to zero demonstrate that the IM does not have any significant impact on the demand estimation, representing an impractical IM. On the other hand, higher values of b indicate a strong dependency between the IM and demand of the structure.

3.3. Proficiency

In order to combine the previous two features, Padgett et al. [3] suggested proficiency, ξ , which is the composite measure of both efficiency and practicality, as follows:

$$\xi = \frac{\beta_{D|IM}}{b} \quad (5)$$

Lower values of ξ indicate more proficient IMs, which have stronger correlation between the IM and the demands while leading to less dispersion around the median values.

3.4. Sufficiency

Sufficiency is defined to evaluate the dependency of the IM to ground motion parameters such as magnitude (M_w) and source-to-site distance (R_d). A sufficient IM should be conditionally independent of such characteristics. The sufficiency of an IM is investigated by conducting a regression analysis on the residuals between the actual response and the estimated demand from the PSDM relative to the ground motion characteristic, M_w or R_d . Generally, the p -value [19] from the regression of the residuals is used to quantify the sufficiency of the IM, which indicates the probability of rejecting the null hypothesis that the slope of the linear regression is zero. Significance levels of 0.1, 1, and 5% are generally used in previous studies as the threshold for IM sufficiency evaluation. Values smaller than the threshold for the linear regression of the residuals on M_w or R_d are an indicator of statistically significant coefficients for the regression estimate, thereby indicating an insufficient IM.

3.5. Hazard computability

As noted, the PSDM relates the demands of the structure to the seismic hazard of the considered region, which is quantified by the IM. Thus, the probabilistic seismic hazard must be computed with respect to the values dictated by the IM. In this regard, the hazard computability is a metric to determine the level of effort required to conduct the probabilistic seismic hazard analysis for a specific IM [18]. For example, hazard maps are readily available for PGA or spectral acceleration at different discrete periods; nonetheless, other IMs such as spectral acceleration at the natural period require more effort or even structure-specific information for their determination. Therefore, despite having an advantage in terms of features such as efficiency, a particular IM may be less desirable according to hazard computability.

4. Issues with the current framework

In the current framework, the efficiency of the IMs is evaluated by $\beta_{D|IM}$, shown in Eq. (4), which is equal to the mean squared error of the linear regression in estimating the demand parameters. This parameter is not normalized to the range of the demand parameters; thus, although it can be used to investigate the efficiency of the IMs for a single demand, it cannot be used to compare the efficiency of IMs on demands of different structural components or for different types of structures (e.g. bridges and buildings), which may have demands of different magnitudes and/or units. Moreover, as noted, parameter $\beta_{D|IM}$ is equal to the mean squared error of the linear regression. Although it is a good estimator of the accuracy of the model, it does not tell anything about the correlation between the estimates from the PSDM and the observed values from the time-history analysis.

Furthermore, practicality of the IM is determined by the slope of the linear regression which is controlled by parameter b in Eq. (3). Although this feature is to determine the dependency of the IM and demand of the structure, it is not a fair comparison if it is used to compare different IMs with different ranges and magnitudes. In fact, as seen in Fig. 1, parameter b (the slope of the fitted linear regression) depends on the range of variables in the x- and y-axis (IM and demands, respectively). While the demand parameter is similar for investigating different IMs for a single component, the IMs can have different ranges, which may affect the slope and therefore the values of parameter b . However, the IMs correspond to the same ground motion database. Therefore, if it is assumed that a suitable ground motion database is used for time-history analyses, the range of IMs should not adversely impact their selection as the practical IM.

Moreover, the proficiency feature (composite of efficiency and practicality), which is the metric that is generally used to determine the optimal IM, also depends on the slope of the linear regression. Therefore, considering slope as an indicator of practicality of the IM

may mislead the outcomes of the optimality investigation. Such a bias in determining the practicality and proficiency criteria may prevent certain IMs with large ranges from being selected as the optimal IM. It is also worth noting that since the practicality and proficiency of the IMs depend on the slope of the linear regression, they cannot be used as evaluation metrics for optimal intensity measure selection when non-linear models are used to estimate the median demand values given IMs in natural log space.

5. Updated framework

In the following section, alternative solutions are suggested to address the abovementioned issues with the current framework.

5.1. Efficiency

In order to make the efficiency metric comparable for different demand parameters with different units and ranges, the following parameter is introduced to evaluate the efficiency of the IMs:

$$\beta_r = \frac{\beta_{D|IM}}{l} \times \frac{1}{1+R} \quad (6)$$

where β_r is the updated parameter to investigate efficiency of the IMs; l is the range of demand parameters in the natural log space, shown in Fig. 2; R is the correlation coefficient [20] between the measured and predicted demand parameters. Larger values of R (closer to 1) represent stronger linear correlation between the demand values and their estimates from the linear regression. As seen in Eq. (6), β_r is a composite of the mean squared error and correlation coefficient of measured and predicted variables, leading to more accurate evaluation of the efficiency of the IMs. Lower values of β_r indicate more efficient IM the PSDM of which has higher predictive power and provides stronger correlation between the demands and their predicted values.

Moreover, normalizing $\beta_{D|IM}$ by the range of the demand parameter in the natural log space not only makes this parameter able to be used for determining the efficient IM on a single demand parameter, but also makes it useful for investigating the efficiency of an IM on different components of a system or even different types of systems. It should be noted that R in Eq. (6) does not depend on the magnitude and range of the demand parameter, so there is no need to normalize this parameter in the equation.

5.2. Practicality

To eliminate the impacts of the IM ranges from this metric, an alternative solution for the practicality criterion is proposed. Here, the practicality, α , is defined as follows,

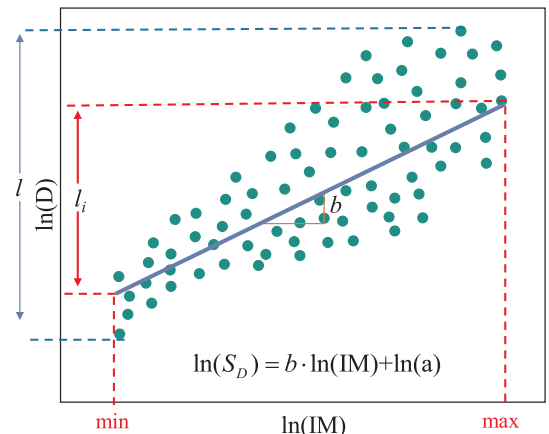


Fig. 2. Illustration of components of parameter α in natural log space.

$$\alpha = \frac{l_i}{l} \tag{7}$$

where l_i is range of the natural log of the demand parameter covered by the PSDM model in the considered range of the IM, and l is the total range of the demand parameter in natural log space. Fig. 2 illustrates the parameters l_i and l in PSDM. As seen in the figure, the practicality, here, is defined as the proportion of the demand range that is covered by the PSDM given the range of the considered IM in the transformed space, l_{IM} . As parameter α increases, the IM becomes more practical. The PSDM for a more practical IM covers a wider range of the demand parameters for the range of the considered IM from the time-history analyses. In fact, demand values are derived from the time-history analyses by subjecting the structures to a set of ground motions with a range of intensities. Thus, to be considered practical, the PSDM for the considered range of IM should represent the entire range of the demand values. Otherwise, the IM is not practical since the PSDM related to that IM does not represent the whole range of demand values observed from time-history analyses. However, unlike the previous metric (i.e., the slope of the linear regression), this parameter does not depend on the magnitude of the considered IMs and demand parameters.

It is worth noting that, according to Eq. (8), parameter α is equal to the slope of the regression line when both $\ln(IM)$ and $\ln(D)$ are normalized by their range, which is shown by parameter b_n in Fig. 3.

$$b_n = \frac{\frac{l_i}{l}}{\frac{[\ln(IM)]_{max}}{l_{IM}} - \frac{[\ln(IM)]_{min}}{l_{IM}}} = \frac{\frac{l_i}{l}}{\frac{1}{l_{IM}}([\ln(IM)]_{max} - [\ln(IM)]_{min})}$$

$$= \frac{\frac{l_i}{l}}{\frac{1}{l_{IM}} \times l_{IM}} = \frac{l_i}{l} = \alpha \tag{8}$$

This normalization before fitting the linear regression diminishes the impacts of the range of the IM and demand parameters on the optimality investigation. Therefore, this parameter can be used to investigate the practicality of different IMs on different components of a system or even different types of systems.

It should be noted that if practicality of two IMs with similar ranges are investigated, the parameter α acts in the same fashion as parameter b , i.e. the slope of the PSDM. That is, the IM corresponding to a higher slope is the one that covers a wider range of demand parameters, leading to larger values for parameter α . However, for nonlinear PSDMs, parameter α from Eq. (7) can be also used as the metric of practicality evaluation when nonlinear models are used to develop PSDMs.

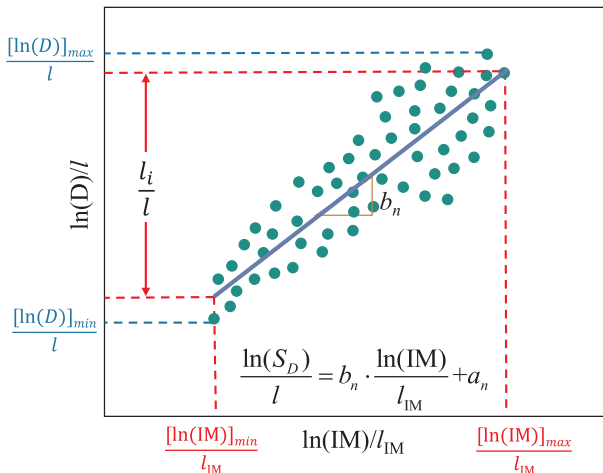


Fig. 3. Illustration of linear regression fitted to $\ln(D)$ and $\ln(IM)$ when they are normalized by their range.

5.3. Proficiency

In the proposed framework, the parameter ξ , which represent the proficiency of the IMs, is also updated as follows,

$$\xi_r = \frac{\beta_r}{\alpha} \tag{9}$$

where ξ_r is still the composite of efficiency and practicality, but the proportion of β_r over α is used to determine the proficiency of the IM. Similar to ξ , lower values of ξ_r indicate a more proficient IM. Moreover, since both components of ξ_r (i.e. β_r and α) are independent of the range of the IMs and range of the demand parameters, ξ_r , similar to efficiency and practicality indexes, can be used for comparing the proficiency of different IMs for different demand parameters and different structural systems.

It should be noted that, in the updated framework, the sufficiency and hazard computability metrics remain unchanged; thus, their features are not discussed in this section.

6. Case study: Modeling and assumptions

The evaluation of intensity measure selection for seismic demand predictions is presented here for multi-span continuous steel girder bridges, hereafter referred to as steel girder bridges for brevity, in the state of Texas. Steel girder bridges make up approximately 11% of the highway bridge inventory of the state [6,21]. The seismic performance of these bridges is of interest due to the recent increase in the seismicity rate in Texas and surrounding associated with more intense natural gas and petroleum production and wastewater injection practices since 2008 [7–11]. Such activities increase the pore pressure, facilitating the release of stored tectonic stress along an adjacent fault. Literature showed that since such earthquakes generally occur at shallow depths, they are likely to have large ground-motion amplitudes, especially at short hypocentral distances [22–25], which could cause damage to the surrounding infrastructure. The 2011 Prague, OK earthquake with moment magnitude, M_w , of 5.7, the 2012 Timpson, TX earthquake with M_w of 4.8, and the 2016 Pawnee, OK earthquake with M_w of 5.8 are three examples of recent seismic events in the area that were reported to cause damage to nearby infrastructure [26–28]. In the following section, the ground motion database, bridge characteristics, and numerical modeling are discussed.

6.1. Ground motion database

This study is motivated by the recent increase in human-induced earthquakes in Texas and surrounding regions. Given the lack of historical data of induced earthquakes specifically in Texas, a database of 200 ground motions corresponding to 36 different seismic events from Texas, Oklahoma, and Kansas from 10/13/2010 to 11/7/2016, was used to represent potential seismic hazards in Texas. These ground motion recordings are selected from a larger database described in Khosravikia et al. [6], which consists of 4500 ground motion recordings from 274 earthquakes happening in the same region since 2005. While the original database intentionally did not distinguish between natural and induced ground motions, the selected ground motions have been classified as induced earthquakes [7,8]. The selected database consists of 50 recordings within each of 4 magnitude bins (i.e., $4.0 \leq M_w < 4.5$, $4.5 \leq M_w < 5.0$, $5.0 \leq M_w < 5.5$, and $M_w \geq 5.5$). The maximum recorded PGA of these ground motions is 0.6 g, recorded at a hypocentral distance, R_{hyp} , of 5.2 km during the 2016 Cushing, Oklahoma event with magnitude of 5.0. Fig. 4 shows the magnitude versus source-to-site distance relation of the considered ground motions.

In addition, Fig. 5 demonstrates the response spectra of the selected ground motions for different peak ground acceleration bins as: $PGA < 0.05$ g, $0.05 \leq PGA < 0.1$ g, $0.1 \leq PGA < 0.3$ g, and

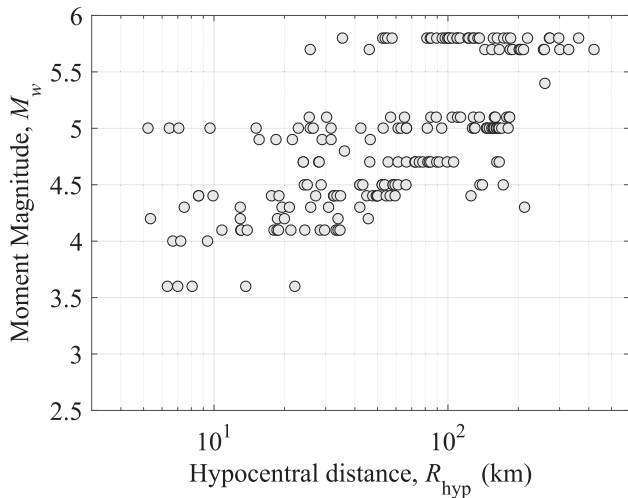


Fig. 4. Magnitude versus hypocentral distance of the considered ground motions.

PGA > 0.3g. The red line in each plot of Fig. 5 demonstrates the median response spectra of the recordings for a specific PGA bin. Moreover, in each plot, the generalized response spectra representative of seismic hazards in different distinct regions of Texas state are also

Table 1

Estimated values of S_S and S_1 from USGS one-year hazard maps representing 1 percent probability of exceedance in 1 year [11] for different regions of Texas.

	Dallas	West Texas	Rest of Texas
S_S (g)	0.18	0.35	0.05
S_1 (g)	0.025	0.035	0.01

shown as a reference.

The generalized response spectra for different regions of Texas are here developed using the spectral accelerations at a period of 0.2 sec and 1.0 sec (S_S and S_1 , respectively), which are determined from the USGS one-year hazard maps representing a 1 percent probability of exceedance in 1 year [11]. The shape of the response spectra between these points was generated following the design spectrum shape defined in the International Building Code (IBC). The seismic hazard in Texas is not uniform; thus, three separate target response spectra are developed for the Dallas-Fort Worth area, for West Texas, and for the rest of Texas. The values of S_S and S_1 for each region are shown in Table 1.

As can be seen in Fig. 5, the selected ground motions cover the range of seismic hazards in the state. They include ground motions representing the low seismicity of much of the state, as represented by the “Reference – Rest of Texas” response spectra at the ground motions with PGA less than 0.05 g, as well as the ground motions that are representative of the more seismically active regions of Dallas and West

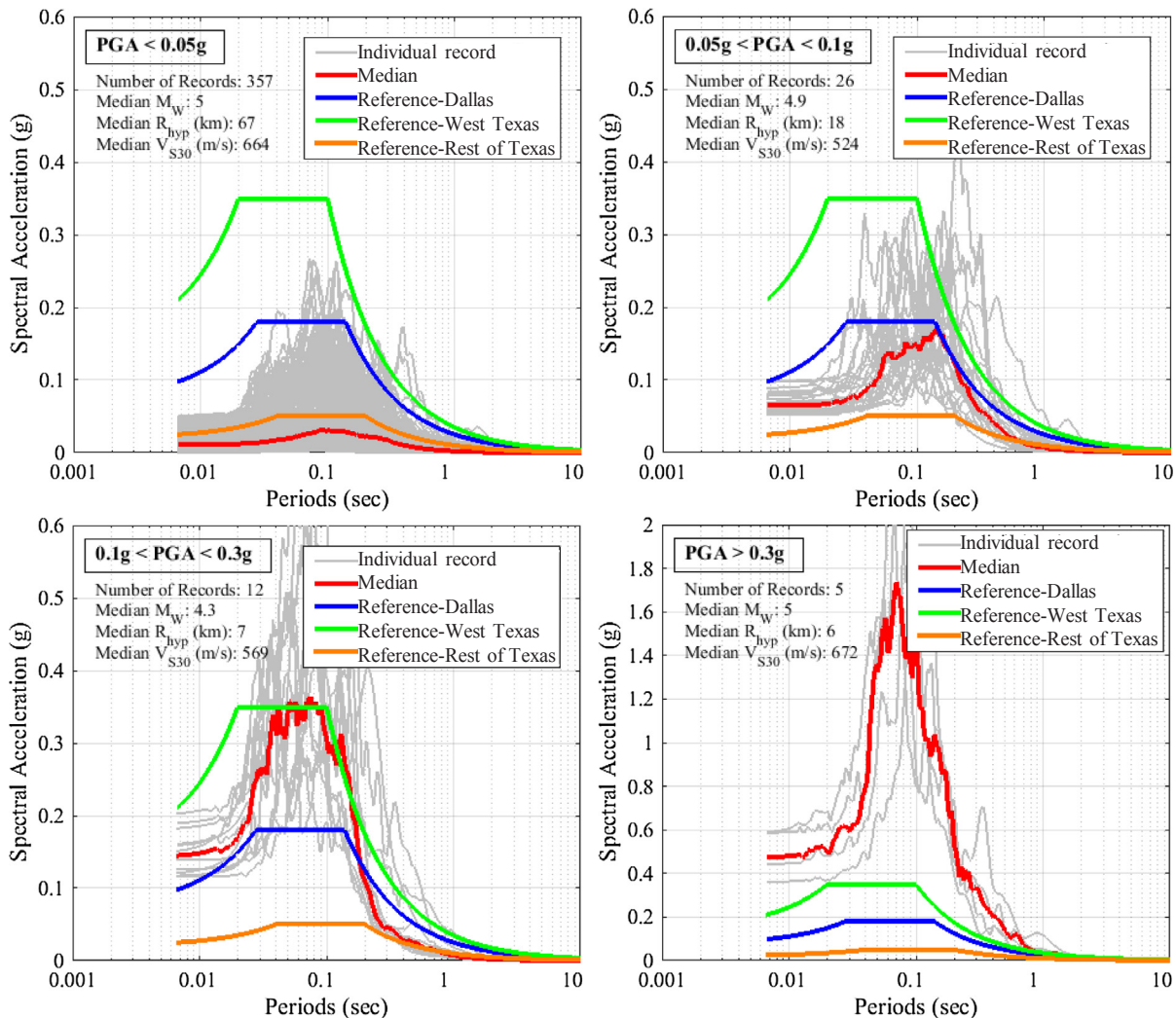


Fig. 5. Response spectra of the selected ground motions for different bins of PGA values [6].

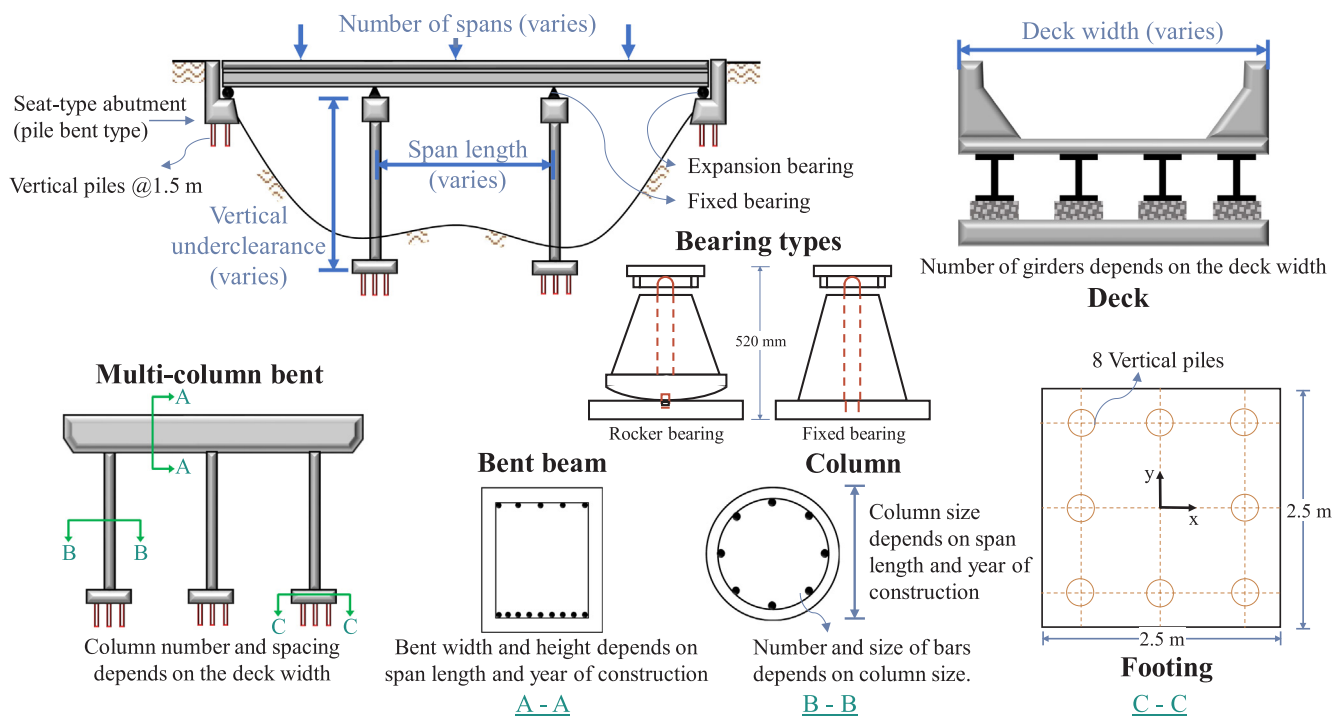


Fig. 6. Schematic view of multi-span continuous steel girder bridges in Texas.

Texas. The selected ground motions also include some motions with response spectra that exceed the reference spectrum for West Texas (e.g. those shown with PGA greater than 0.3 g) to represent the upper bound of ground shaking expected in Texas.

6.2. Bridge characteristics and modeling

Fig. 6 shows a schematic view of multi-span continuous steel girder bridges, which are referred to herein as steel girder bridges. Khosravikia et al. [21] showed that steel girder bridges were most popular in the 1960s in Texas. As noted, Texas had a very low historic seismicity, and therefore, most of the bridges were designed with little to no consideration of seismic demands. According to the Texas Department of Transportation (TxDOT) bridge database, the majority of steel girder bridges (i.e. over 70%) are supported by multi-column bents. Thus, multi-column bents are considered as the bent type in the analyses for these bridges. As seen in the figure, the column diameter is typically governed by span length and year of construction. Investigation of TxDOT standard drawings and as-built bridge drawings from the 1930s to 2000s indicated that TxDOT multi-column bents have historically utilized either 24-inch diameter or 30-inch diameter columns. The specific column sizes and details used for each bridge class are found in Khosravikia et al. [6].

Review of as-built bridge drawings indicates that most of the steel girder bridge inventory in Texas built prior to the 1990s, which consist of high-type steel expansion (rocker) and fixed bearings, as shown in Fig. 6. A fixed bearing can accommodate rotational movement, while an expansion bearing allows both rotation and horizontal translation in the longitudinal direction. Moreover, review of TxDOT standard and as-built drawings indicates that most bridges have pile-bent seat abutments that have two types of resistance in the longitudinal direction as: (1) Passive resistance, which is developed as a result of pressing the abutment into the soil. In this case, both the soil and the piles beneath the abutment provide resistance. (2) Active resistance, which is developed as a result of pulling the abutment away from the backfill. In this case, resistance is only provided by piles beneath the abutment. It is worth noting that for the transverse direction, only the piles are

assumed to contribute to the resistance. Furthermore, it is observed that the majority of bridges (about 75%) have no or very little skew (less than fifteen degrees), which is defined as the angle between the centerline of supports and a line perpendicular to the centerline of the roadway. According to Sullivan and Nielson [29], a skew angle less than fifteen degrees has little to no effect on seismic vulnerability of a bridge; therefore, skew is neglected in this study.

The main bridge parameters that affect seismic performance and modeling are number of spans, span length, vertical underclearance, and deck width. Vertical underclearance refers to the total height of the column, bearing, and bent cap, which can be used as a proxy for estimating column height in the numerical bridge models. The probability distributions of these parameters are extracted from the FHWA National Bridge Inventory (NBI) [30] and Texas Department of Transportation (TxDOT) bridge database and are shown in Fig. 7. As seen, 80% of the bridges in this class consist of less than six spans, the lengths of which typically vary between 5 m and 60 m. The vertical underclearance of these bridges also varies between 3.9 m and 7.6 m, and their decks have widths ranging from 6 m to 30 m. The average of each parameter is also shown in Fig. 7.

Based on the abovementioned distributions, eight bridge configurations are sampled using the Latin Hypercube Sampling method from the population of the bridge class inventory to account for the variability of geometry and date of construction. According to Huntington and Lyrintzis [31], Latin Hypercube Sampling (LHS), which utilizes a stratified random sampling technique, is a variant of Monte Carlo that utilizes relatively smaller samples. In this approach, the cumulative distribution function for the parameters of interest are divided into the desired number of equal sections or bins, and then, a sample is randomly selected from each bin. This approach allows for the full probabilistic distribution to be represented in just a small number of samples.

It is worth noting that the distributions of some geometric variables are modified before sampling to reduce unnecessary complexities in the modeling process. For example, there are some bridges in the population that have a very large number of spans (e.g., 12 or more). In such cases, LHS could generate samples with a similarly large number of

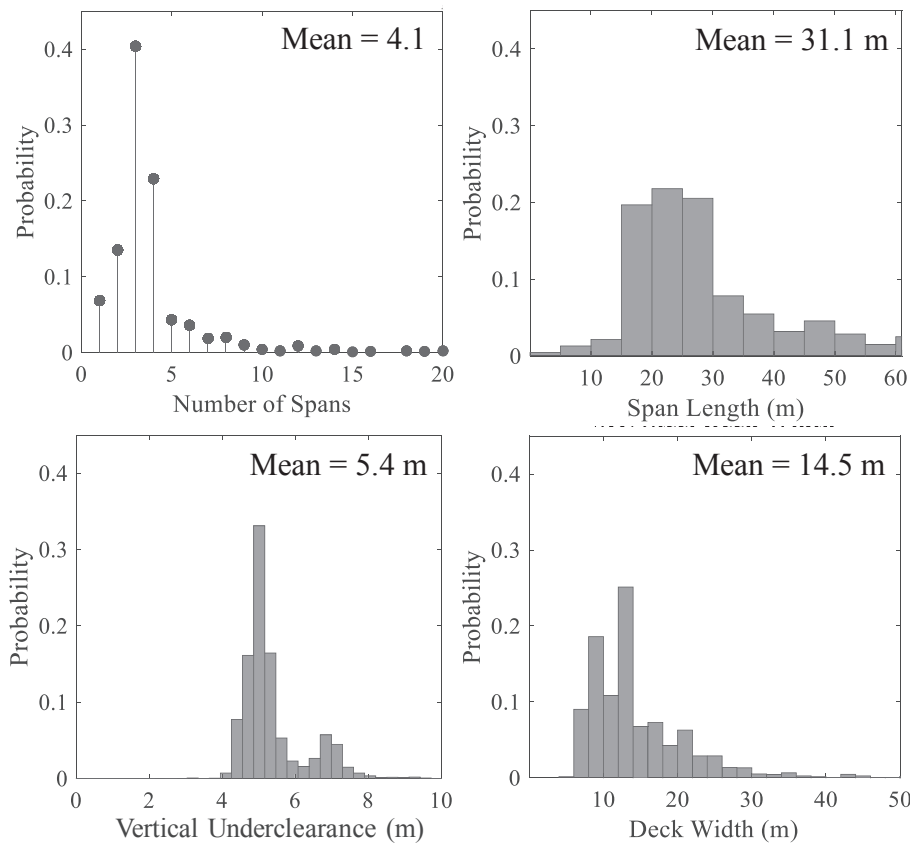


Fig. 7. Geometric characteristics of multi-span continuous steel girder bridges in Texas.

spans which would significantly increase the computational expense during the nonlinear response-history analyses. On the other hand, for such cases, the expected damage is not expected to be substantially different from a bridge with significantly fewer spans [29]. Thus, in this study, the number of spans considered in the sampling methods are reduced to only two to five span configurations to avoid having models with an excessive number of spans. This range of spans covers over 70% of the steel girder bridge population in Texas. Moreover, to ensure that the bridge samples capture the vast majority of the bridge inventory without generating unnecessarily complex and computationally expensive bridge models, the deck width and span length are sampled from the 10th to the 90th percentile of the inventory.

In the sampling procedure, the correlations among the geometric parameters are also taken into account to ensure that the combination of the sampled geometric parameters represents the inventory. The correlations are computed based on the information derived from constructed bridges and are available at Khosravikia et al. [6]. The geometric parameters of each bridge configuration are shown in Table 2. As seen in the table, the bridge configurations have two to four

spans with lengths between 12.2 m and 73.2 m.

In addition, the uncertainty in material properties is also taken into account by considering them as random variables. The details of the distribution type assigned for the material properties, as well as other key modeling parameters (e.g. damping ratio and loading direction) are shown in Table 3. The ranges and statistics of these parameters come from the TxDOT and NBI databases [30] as well as other relevant studies in the Central and Eastern U.S. [32]. To properly account for the effect of the uncertainty in material properties of each bridge configuration, eight different bridge samples with different material properties are randomly generated for each bridge configuration using the LHS method, resulting in 64 total bridge samples.

The behavior of the 64 bridge samples are simulated in the *OpenSees* analysis program [33] using three-dimensional (3D) models. The software provides robust nonlinear dynamic analysis capabilities with numerous built-in and user-defined materials to represent a wide range of nonlinear behaviors. Fig. 8 shows the three-dimensional numerical model of bridge system that was developed for this study. As seen in the figure, the developed model contains beam-column elements for the columns, bent caps, and girders, with concentrated translational and/or rotational springs to simulate nonlinearity. For these models, it is assumed that the bridge deck and girders behave elastically with no damage. This assumption is consistent with past studies and post-earthquake inspections [34,35]. Nielson and DesRoches [34] modeled the bridge girders and deck as a single beam with stiffness properties determined from the composite multi-girder and deck section. The present study employs a more detailed grid of beam elements to better model the vertically and horizontally distributed stiffness and mass of the girder and deck system, similar to the grid model described in Filipov et al. [35]. A brief description of the numerical modeling procedure for each component of the bridges is provided in the following paragraphs. However, for full details of the numerical models, see the work done by

Table 2

Geometric parameters of representative bridge configurations.

Bridge no.	Spans	Span length (m)	Deck width (m)	Vertical underclearance (m)
1	3	18.20	20.10	6.65
2	4	27.43	8.50	4.98
3	3	26.52	9.51	4.44
4	4	35.97	16.37	4.22
5	3	12.19	12.63	4.90
6	4	44.20	13.17	4.65
7	3	21.34	12.19	4.72
8	2	73.15	10.73	5.28

Table 3
Summary of modeling parameters and distribution characteristics.

Modeling parameter	Distribution	Probability Parameters		Units
		a^1	b^1	
Concrete strength	Normal	29.0	5.9	Mpa
Reinforcing strength	Lognormal	379	34	Mpa
Steel fixed - longitudinal	Uniform	74.4	111.6	kN/mm
Steel fixed - transverse	Uniform	4.0	6.0	kN/mm
Steel fixed COF ² -longitudinal	Uniform	0.168	0.252	
Steel fixed COF ² -transverse	Uniform	0.296	0.444	
Steel rocker COF ² -longitudinal	Uniform	0.032	0.048	
Steel rocker COF ² -transverse	Uniform	0.080	0.120	
Abutment - passive stiffness	Uniform	11.5	28.7	kN/mm/m
Pile stiffness	Uniform	3.5	10.5	kN/mm per pile factor
Superstructure mass	Uniform	1.1	1.4	
Damping ratio	Normal	0.05	0.01	
Deck gaps	Uniform	25	152	mm
Loading direction	Uniform	0	360	degrees

¹ For normal and lognormal distributions, a and b indicate the median and dispersion, respectively, and for uniform distribution, a and b represent the lower and upper bounds, respectively.

² COF: Coefficient of friction.

Khosravikia et al. [6].

For columns, flexural and/or combined axial-flexural damage are commonly observed in earthquakes; however, columns in low-seismic regions may also be more susceptible to shear failure modes due to the poor confinement and shear reinforcement found in non-seismically detailed columns. In this study, a concentrated plasticity model is used to model nonlinear column behavior. Columns are modeled as elastic beam-column elements with nonlinear rotational springs (i.e., zero-length elements) at the top and bottom acting in two orthogonal directions (i.e. longitudinal and transverse). Each spring is assigned a nonlinear moment-rotation behavior to capture flexure, shear, and lap splice failures in columns based on the backbone strength parameters presented in ACI [36] and ASCE/SEI 41-17 [37]. The nonlinear hysteretic behavior of the rotational springs was calibrated per a large database of 319 and 171 rectangular and circular columns, respectively, that were tested under cyclic loading with various levels of seismic detailing and shear reinforcement [38,39]. More details of the column numerical modeling and experimental validation are available at

Khosravikia et al. [6].

Bearings are another component that can significantly affect bridge seismic performance. As previously discussed, the steel girder bridges in this study employed steel bearings. For such bearings, nonlinear models under lateral loads are developed and calibrated with extensive experimental data available in the research literature [40]. For other components such as expansion joints, deck pounding, abutments, and foundations, nonlinear models developed in previous studies [34,35,41] are assigned. However, such models are adjusted with appropriate modifications to represent typical details of Texas bridge infrastructures.

The natural periods of the 64 sampled bridges vary between 0.3 and 0.8 s, which respectively correspond to the bridge configurations with shortest and longest span lengths. Moreover, it is worth noting that by looking into the mode shapes of the bridges, it is found that the longitudinal translation mode is the fundamental mode for the majority of the bridge samples, which is consistent with previous relevant studies such as Nielson [42] and Padgett et al. [3]. This observation is mainly because of the fact that, as shown in Fig. 6, most of the steel girder bridges in Texas consist of multi-column bents, which provide much more stiffness in the transverse direction compared to the longitudinal direction. In addition, having expansion bearings, which allows for more deformation in the longitudinal direction, as well as gaps between abutments and girders in the longitudinal direction increase the fundamental period of the bridges in this direction.

The nonlinear 3D model of each of the 64 bridges, shown in Fig. 8, is subjected to 10 randomly selected ground motions that are scaled to different values of spectral acceleration at the bridge’s natural period, varying between 0.2 and 2 g with increments of 0.2 g, which leads to 640 nonlinear response-history analyses. In this study, it is assumed that damage can occur in columns, bearings, and abutments; therefore, the responses of these components are recorded during each analysis. In particular, for column response, the maximum rotation in the column hinge is captured. For bearings, the longitudinal and transverse deformations of both fixed and expansion bearings are recorded during the analyses. Finally, for abutments, deformations in passive, active, and transverse directions are documented. The list of the demand parameters considered in this study is shown in Table 4. These outputs are set as inputs for the probabilistic seismic demand models, which are discussed in the next section.

6.3. Probabilistic seismic demand models

As noted, probabilistic seismic demand model (PSDM) predicts the demand of the structure given the IM of the ground motion and is based

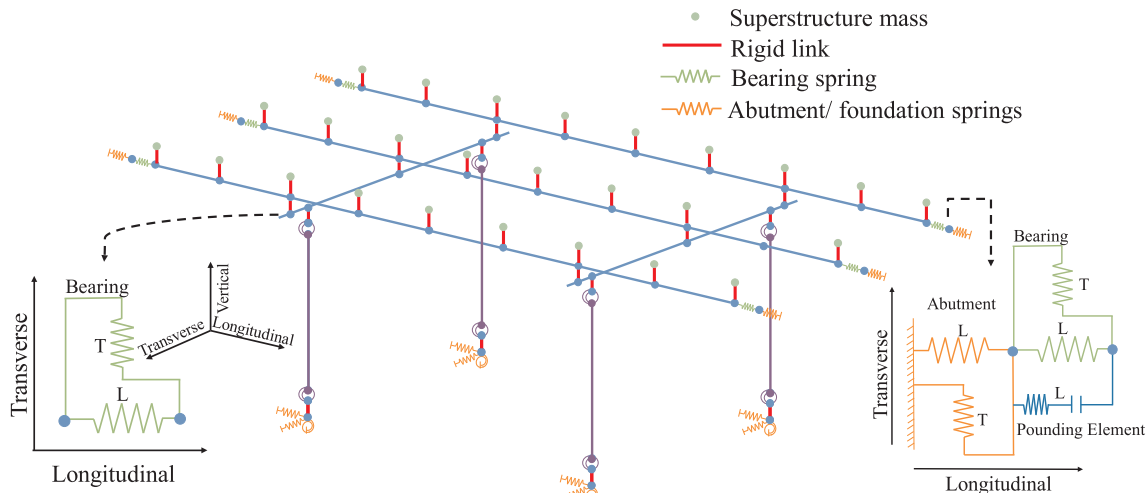


Fig. 8. Schematic view of the 3D bridge model.

Table 4
Demand parameters of different bridge components considered in this study.

Demand parameter	Abbreviation	Units
Column rotation	Rot	rad
Fixed bearing: Longitudinal deformation	fx_L	mm
Fixed bearing: Transverse deformation	fx_T	mm
Expansion bearing: Longitudinal deformation	ex_L	mm
Expansion bearing: Transverse deformation	ex_T	mm
Abutment: Active deformation	abut_A	mm
Abutment: Passive deformation	abut_P	mm
Abutment: Transverse deformation	abut_T	mm

Table 5
Considered intensity measures.

Intensity measure	Description	Units
PGA	Peak Ground Acceleration	g
PGV	Peak Ground Velocity	mm/s
PGD	Peak Ground Displacement	mm
$S_a(T_n)$	Peak Spectral Acceleration at natural period, T_n	g
$S_a(0.2\text{ s})$	Peak Spectral Acceleration at 0.2 s	g
$S_a(1.0\text{ s})$	Peak Spectral Acceleration at 1.0 s	g
I_a	Arias Intensity	mm/s

on the results from the nonlinear response-history analyses. In this study, PSDMs are developed for the demand parameters presented in Table 4. To investigate the optimality of IMs, seven different IMs (shown in Table 5) are considered for development of the PSDMs, including acceleration-related IMs (e.g. PGA and I_a), velocity-related IMs (e.g. PGV), displacement-related IMs (e.g. PGD), and structure-specific IMs (e.g. S_a at 0.2 s, and 1.0 s, and the natural period of the bridges, T_n).

For each pair of demand-IM, the PSDM is developed by fitting a linear regression to the results from nonlinear response-history analyses to compute the coefficients a and b in Eq. (3), and computing the dispersion of the data around the fitted line, $\beta_{D|IM}$, using Eq. (4). Table 6 presents the parameters of the PSDMs (a , b , and $\beta_{D|IM}$), for the four demand parameters including column rotation (Rot), longitudinal deformations of fixed and expansion bearings (fx_L and ex_L, respectively), as well as transverse deformation of the abutment (abut_T).

7. Discussion of the IM selection

In this section, first, both current and updated frameworks are applied to the considered case study to comparatively investigate the differences in conventional and proposed IM evaluation metrics. Then, using the proposed framework, the optimality of IMs for steel girder bridges in the state of Texas are discussed. This information can be used in further research for more reliable performance predictions of the bridge infrastructure in this area subjected to human-induced seismicity.

Table 6
PSDMs for four different demand parameters considering different IMs.

IM	Rot			fx_L			ex_L			abut_T		
	a	b	$\beta_{D IM}$	a	b	$\beta_{D IM}$	a	b	$\beta_{D IM}$	a	b	$\beta_{D IM}$
PGA	0.00	1.05	1.02	2.54	0.77	0.94	30.37	0.68	0.71	10.19	0.61	0.92
PGV	0.00	1.48	0.73	0.01	0.94	0.92	0.12	0.96	0.53	0.08	0.85	0.82
PGD	0.00	0.69	1.24	0.43	0.40	1.14	3.35	0.49	0.80	1.76	0.39	1.01
$S_a(0.2\text{ s})$	0.00	1.18	0.95	1.66	0.77	0.99	19.65	0.76	0.67	6.76	0.71	0.87
$S_a(1.0\text{ s})$	0.04	1.37	0.76	10.31	0.75	1.02	159.28	0.92	0.50	39.82	0.75	0.86
$S_a(T_n)$	0.01	1.65	0.94	4.23	1.12	0.95	48.60	1.06	0.66	14.00	0.61	1.03
I_a	0.00	0.56	0.92	0.06	0.40	0.95	0.98	0.38	0.67	0.52	0.33	0.91

7.1. Comparison of conventional and proposed frameworks

Fig. 9 shows the efficiency, practicality, and proficiency of the considered IMs for four different demand parameters of steel girder bridges listed in Table 6 using both conventional and updated frameworks. As seen in Fig. 9, for a specific demand parameter, using both frameworks leads to a similar order for the efficiency of the IMs, where lower values indicate more efficient IMs. For example, regardless of the framework, the order of PGV, $S_a(1.0\text{ s})$, I_a , $S_a(T_n)$, $S_a(0.2\text{ s})$, PGA, and PGD, from most to least efficient are determined for column rotation. However, there are two key differences between the efficiency results from conventional and proposed frameworks as follows:

First, the $\beta_{D|IM}$ values from the conventional framework may be misleading when they are used for investigating efficiency of IMs for different demand parameters. For example, the PSDM corresponding to the column rotation demand given PGA provides a larger value of $\beta_{D|IM}$ compared to the relevant PSDM for longitudinal deformations of fixed bearing given the same IM, simply due to the magnitude of values observed for each of these demands. However, the suggested index for efficiency evaluation (i.e. β_r) demonstrates that it does not necessarily mean that the conditional PSDM for columns upon PGA is less accurate than that developed for bearings. In fact, the values of β_r indicate that conditional PSDM upon PGA developed for column provides much stronger predictive power than that of longitudinal deformation of fixed bearings.

Moreover, the values from the proposed framework provide more accurate estimations of the efficiency feature of the IMs, because they consider both dispersion and correlation among the predicted and measured data. For example, for longitudinal deformation of the fixed bearing (i.e. fx_L), the conventional framework suggested values of 1.17 and 0.96 for PGD and $S_a(0.2\text{ s})$, respectively. That is, $S_a(0.2\text{ s})$ provides 13% lower $\beta_{D|IM}$ comparing to PGD for this specific demand parameter. However, for the same demand parameter, the proposed framework provides approximately 26% difference between the efficiency index of PGD and $S_a(0.2\text{ s})$, which indicates that $S_a(0.2\text{ s})$ is much more efficient than PGD. This observation is mainly because of the fact that $S_a(0.2\text{ s})$ provides not only lower dispersion (i.e. $\beta_{D|IM}$) but also a higher correlation coefficient (i.e. R) compared to PGD for the considered demand parameter. However, for column rotation (i.e. Rot), the conventional framework suggests that PGV is much more efficient than PGA. Although a similar order is also observed in the proposed framework, a smaller difference is observed for the efficiency index of these IMs, which is mainly because of the fact that PGA provides slightly larger values of R compared to PGV for column rotation. Therefore, both dispersion and correlation coefficient are key parameters in determining the accuracy of the PSDM developed for a specific demand parameter, and they both are taken into account in the proposed efficiency index.

Considering practicality of the IMs, regardless of the demand parameter of interest, the conventional framework suggests that I_a is the least practical IM among others. This observation is mainly because of the differences in the range and magnitude of the considered IMs. For

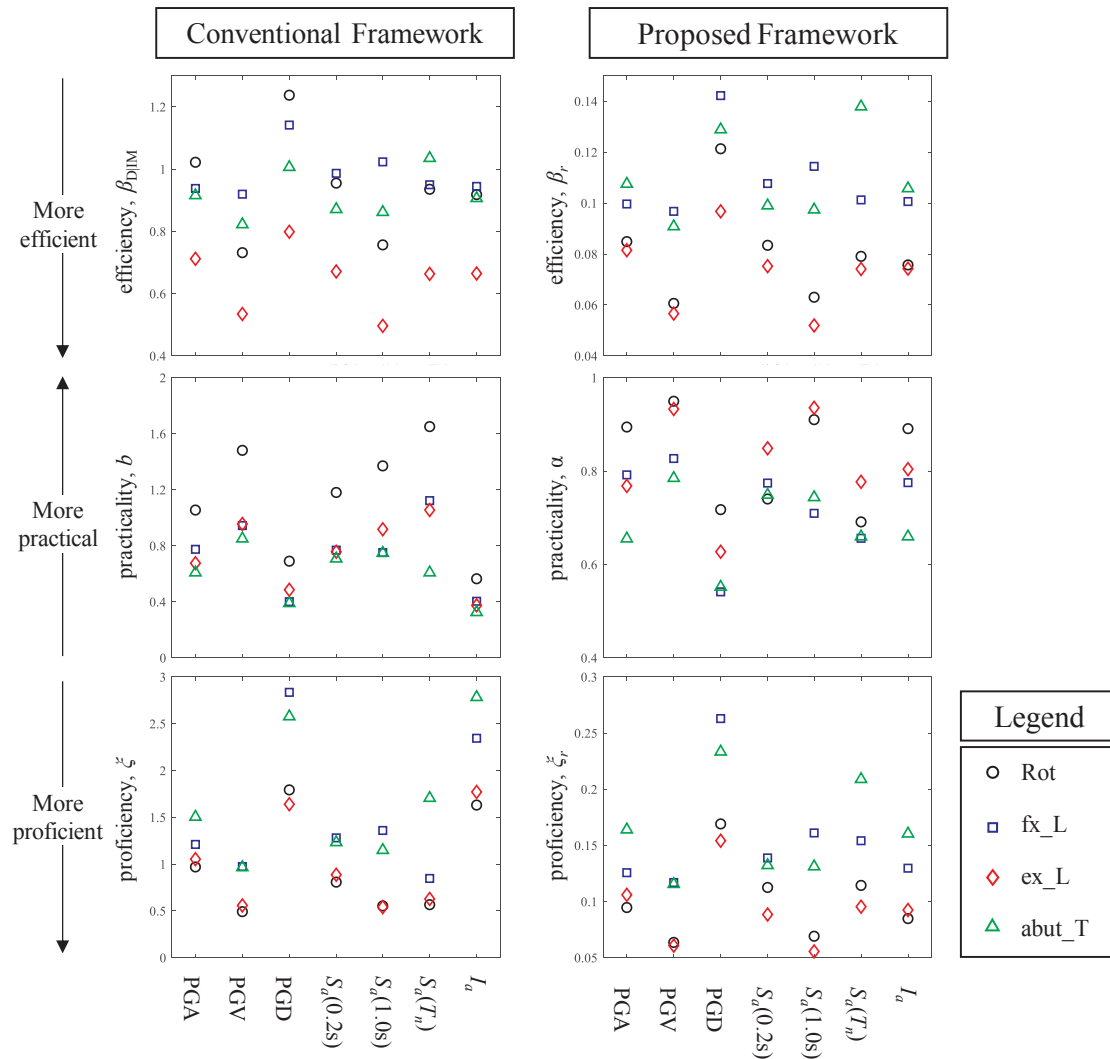


Fig. 9. Efficiency, practicality, and proficiency evaluation of the considered IMs for steel girder bridges with conventional and proposed framework.

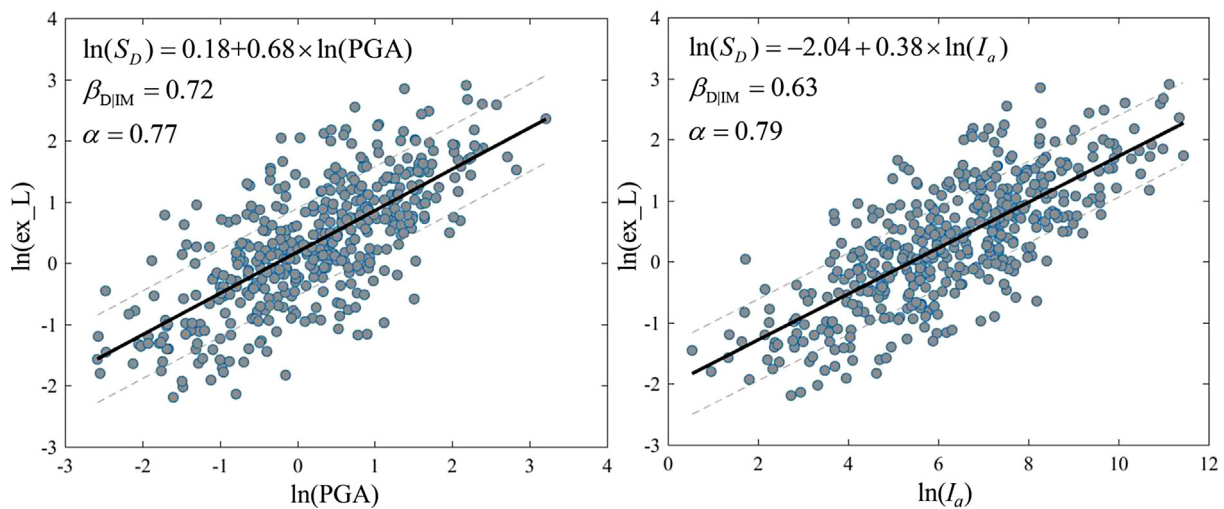


Fig. 10. PSDMs of longitudinal deformation of expansion bearings, ex_L , considering PGA and I_a .

illustration, Fig. 10 shows the values of the longitudinal deformation of the expansion bearings, ex_L , of the steel girder bridges given PGA and I_a . The results in the figure correspond to the same response-history analyses, and therefore, both plots contain the same range of demand

values (y-axis). As seen in the figure, since I_a contains a wider range of values, it corresponds to a lower slope (b values), and therefore, it is less practical when the slope of the IM is used as the metric to investigate the practicality of the IMs. This observation can also be found in other

studies because the slope, here, only depends on the range of the IM, and I_a always contains a wider range, which indicates the bias in the practicality investigation. For example, in the study conducted by Padgett et al. [3] about the selection of an optimal IM for bridge portfolios, while I_a was the most efficient parameter for most of the bridge demand parameters, it led to a much lower slope, making it a much less practical and proficient IM. However, the values of α , shown in Fig. 10, demonstrates that the PSDM for I_a covers a wider range of the observed demand parameter, and hence, it is more practical compared to PGA. The same trend is observed if the natural log of the IMs is normalized before fitting the linear regression to the models. It should be noted that IMs like I_a may not be the optimal IM because of hazard computability or sufficiency features; however, it should not be reflected when the practicality of the IMs are evaluated.

The change in the practicality order is also reflected in the proficiency of the IMs. In fact, as seen in Fig. 9, according to the conventional framework, for longitudinal deformation of the expansion bearing, $S_a(0.2\text{ s})$ is a more proficient IM than PGA, which is, in turn, more proficient than I_a . However, in the proposed framework, $S_a(0.2\text{ s})$ and I_a have similar proficiency, which is better than that of PGA. This change in the order of the IM proficiency is due to the elimination of the bias in the IM practicality metric. Moreover, since the practicality and efficiency parameters are normalized to the range of the demand parameters, the values derived for the proficiency index (i.e. ξ_r) for different components are now comparable. For instance, according to Fig. 9, PGA is more proficient in estimating the column responses than those of bearings and abutments.

7.2. Optimal IM selection for steel girder bridges in the state of Texas

Here, the results from the proposed framework are used to determine the optimal IM for steel bridge infrastructure in the state of Texas. Fig. 11 shows the proficiency order of the IMs for different components of the bridges. As seen in the figure, the velocity-related IM (i.e. PGV) and the spectral acceleration at long period (i.e. $S_a(1.0\text{ s})$) are the two most proficient IMs for most of the demand parameters considered in this study. In previous optimal IM studies [3], it was determined that the acceleration-related IM (i.e. PGA) is the most proficient IM for steel bridge portfolios in Central United States. The difference in the proficient IM for steel girder bridges in Texas and Central United States is a key observation in performance-based assessment of infrastructure subjected to potentially induced earthquakes. Further research is required to determine whether it is correlated to geological effects, bridge characteristics, or nature of the induced seismicity.

After these two IMs, spectral acceleration at short periods (i.e. 0.2 s) is the most proficient IM. It is mainly because of the fact that for these

Table 7 Sufficiency evaluation of considered IMs for different demand parameters of steel girder bridges in Texas.

IMs	Rot		fx_L		ex_L		abut_T	
	M_w	R_{hyp}	M_w	R_{hyp}	M_w	R_{hyp}	M_w	R_{hyp}
PGA	0.00	0.00	0.23	0.18	0.00	0.00	0.00	0.00
PGV	0.00	0.00	0.06	0.01	0.00	0.00	0.01	0.00
PGD	0.00	0.02	0.00	0.00	0.00	0.08	0.00	0.09
$S_a(0.2\text{ s})$	0.00	0.00	0.23	0.17	0.00	0.00	0.00	0.00
$S_a(1.0\text{ s})$	0.00	0.00	0.00	0.00	0.00	0.03	0.00	0.08
$S_a(T_n)$	0.60	0.61	0.00	0.00	0.19	0.62	0.45	0.73
I_a	0.00	0.00	0.11	0.23	0.00	0.00	0.02	0.00

ground motions, in which the spectral acceleration diminishes very quickly with period, spectral acceleration at short periods (i.e. 0.2 s) can be a proficient IM for bridge evaluation. It is worth noting that the spectral accelerations at constant periods (i.e. $S_a(0.2\text{ s})$ and $S_a(1.0\text{ s})$) are more proficient than spectral accelerations at natural period of the bridges (i.e. $S_a(T_n)$). Thereafter, acceleration-related IMs (i.e. PGA and I_a) are the next most proficient IMs. Note that I_a is the composite of duration and acceleration time-history; thus, there is a strong correlation between PGA and I_a . This correlation makes them perform in a similar fashion. However, I_a is slightly more proficient since duration of the ground motions are also taken into account in I_a . Finally, Fig. 11 shows that the displacement-related IM (i.e. PGD) is not a proficient IM for seismic performance assessment of steel girder bridges in Texas subjected to potentially human-induced seismic hazard.

In addition, it is worth noting that hazard maps are readily available for PGV and spectral acceleration at constant values (i.e. 0.2 and 1.0 s). Therefore, not only are these IMs the most proficient IMs, but also they have an advantage in terms of hazard computability.

To investigate the sufficiency of the IMs, Table 7 shows the p-values for the residuals of the PSDMs and ground motion characteristics such as magnitude, M_w , and source-to-site distance, R_d . Here, hypocentral distance, R_{hyp} , is considered as an indicator of source-to-site distance. A significance level of 5% is considered in this study as the threshold for IM sufficiency evaluation. As seen in the table, not a single IM passes the sufficiency test for all the demand parameters. The insufficiency of the considered IMs is a motivation for further researches to find an alternative IM to pass the sufficiency test for such earthquakes.

8. Summary and conclusion

The present study evaluates the conventional metrics for selection of the optimal intensity measure, IM, for probabilistic seismic demand models (PSDMs). Such models are critical in relating the seismic hazard and structural responses in probabilistic performance assessments, and selection of an optimal IM is very promising in reducing the uncertainty in the PSDMs and increasing the reliability and usability of the PSDMs for performance-based earthquake engineering analysis. It has been traditionally shown that the demand of the structures follows a linear function of the IM in natural log space; therefore, PSDMs are generally determined by fitting a linear regression to the database in natural log space.

The current study evaluated the metrics as: efficiency, which demonstrates the uncertainty of the PSDM given IM; practicality, which demonstrates the dependency of the demands on the IM; proficiency, which is the composite of efficiency and practicality; sufficiency, which demonstrates the dependency of the outcome to ground motion parameters such as magnitude and source-to-site distance; and finally hazard computability, which demonstrates the amount of effort to extract hazard maps and curves for the considered IM.

The present study shows that the current metric for practicality, which is determined by the slope of the linear regression fitted to the

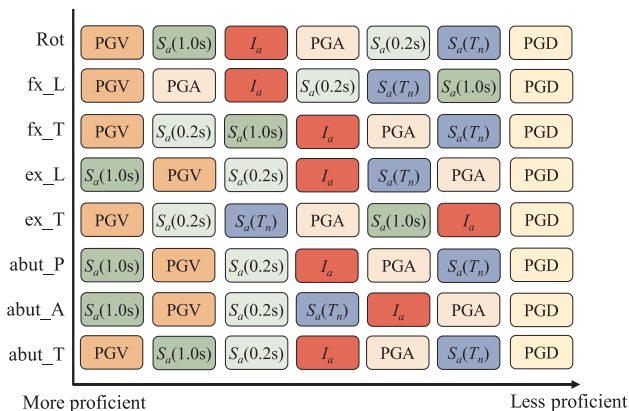


Fig. 11. Proficiency evaluation of considered IMs for different demand parameters of steel girder bridges in Texas.

data may mislead the selection of the optimal IM when IMs with different ranges and magnitudes are investigated. The metric may also adversely affect the proficiency feature which is the composite of efficiency and practicality and is the parameter that is conventionally used to choose the IM with both efficiency and practicality. Moreover, the efficiency metric can produce biased results when evaluating different components or systems that have different magnitudes of demand. Thus, alternative solutions are proposed to investigate the efficiency, practicality, and proficiency features of the IMs, which diminish the impacts of the range of the IMs and demand parameters in these commonly used optimality metrics. The proposed framework can be used for optimal IM evaluation of different types of structures and different forms of probabilistic seismic demand models.

Then, the proposed framework is applied to the steel girder bridge portfolios in the state of Texas, which has been recently subjected to increased seismicity due to human-induced earthquakes starting around 2009. The results show that for this bridge system, the velocity-related IM (i.e. PGV) leads to more accurate estimates of the structural responses, while literature shows that the acceleration-related IM (i.e. PGA) is the most proficient IM for similar bridge systems in other areas of the Central United States.

Declaration of Competing Interest

The authors declare that they have no known competing financial interests or personal relationships that could have appeared to influence the work reported in this paper.

Acknowledgements

This work was financially supported by the Texas Department of Transportation (TxDOT) through Grant Number 0-6916, the state of Texas through the TexNet Seismic Monitoring Project, and the Industrial Associates of the Center for Integrated Seismic Research (CISR) at the Bureau of Economic Geology of the University of Texas. The opinions and findings expressed herein are those of the authors and not the sponsors. The authors also thank Dr. George Zalachoris and Dr. Ellen Rathje from The University of Texas at Austin for providing the ground motion database used in this study.

Appendix A. Supplementary material

Supplementary data to this article can be found online at <https://doi.org/10.1016/j.engstruct.2019.109899>.

References

- Moehle J, Deierlein GG. A framework methodology for performance-based earthquake engineering. Proceedings of 13th world conference on earthquake engineering. Vancouver, BC, Canada. 2004.
- Mackie K, Stojadinović B. Probabilistic seismic demand model for California highway bridges. *J Bridge Eng* 2001;6:468–81.
- Padgett JE, Nielson BG, Desroches R. Selection of optimal intensity measures in probabilistic seismic demand models of highway bridge portfolios. *Earthquake Eng Struct Dyn* 2008;37:711–25.
- Hariri-Ardebili MA, Saouma VE. Probabilistic seismic demand model and optimal intensity measure for concrete dams. *Struct Saf* 2016;59:67–85.
- Wang X, Shafieezadeh A, Ye A. Optimal intensity measures for probabilistic seismic demand modeling of extended pile-shaft-supported bridges in liquefied and laterally spreading ground. *Bull Earthq Eng* 2018;16:229–57.
- Khosravikia F, Potter A, Prakhov V, Zalachoris G, Cheng T, Tiwari A, et al. Seismic vulnerability and post-event actions for Texas bridge infrastructure. FHWA/TX-18/0-6916-1, Center for Transportation Research (CTR); 2018.
- Petersen M, Mueller CS, Moschetti MP, Hoover SM, Llenos AL, Ellsworth WL, et al. 2016 One-year seismic hazard forecast for the central and eastern United States from induced and natural earthquakes. Open-File Report 2016.
- Frohlich C, Deshon H, Stump B, Hayward C, Hornbach M, Walter JI. A historical review of induced earthquakes in Texas. *Seismol Res Lett* 2016;87:1–17. <https://doi.org/10.1785/0220160016>.
- Hornbach MJ, Jones M, Scales M, DeShon HR, Magnani MB, Frohlich C, et al. Ellenburger wastewater injection and seismicity in North Texas. *Phys Earth Planet Inter* 2016;261:54–68.
- Hough SE. Shaking from injection-induced earthquakes in the central and eastern United States. *Bull Seismol Soc Am* 2014;104(5):2619–26.
- Petersen MD, Mueller CS, Moschetti MP, Hoover SM, Shumway AM, McNamara DE, et al. 2017 one-year seismic-hazard forecast for the Central and Eastern United States from induced and natural earthquakes. *Seismol Res Lett* 2017;88:772–83.
- Cornell CA, Jalayer F, Hamburger RO, Foutch DA. Probabilistic basis for 2000 SAC federal emergency management agency steel moment frame guidelines. *J Struct Eng* 2002;128:526–33.
- Cybenko G. Approximation by superpositions of a sigmoidal function. *Math Control Signals Syst* 1992;5(4). <https://doi.org/10.1007/BF02551274>. 455–455.
- Lagaros ND, Fragiadakis M. Fragility assessment of steel frames using neural networks. *Earthquake Spectra* 2007;23:735–52.
- Mitropoulou CC, Papadarakis M. Developing fragility curves based on neural network IDA predictions. *Eng Struct* 2011;33:3409–21.
- Wang Z, Pedroni N, Zentner I, Zio E. Seismic fragility analysis with artificial neural networks: Application to nuclear power plant equipment. *Eng Struct* 2018;162:213–25.
- Luco N, Cornell CA. Structure-specific scalar intensity measures for near-source and ordinary earthquake ground motions. *Earthquake Spectra* 2007;23:357–92.
- Giovenale P, Cornell CA, Esteva L. Comparing the adequacy of alternative ground motion intensity measures for the estimation of structural responses. *Earthquake Eng Struct Dyn* 2004;33:951–79.
- Ang AH-S, Tang WH, et al. Probability concepts in engineering: emphasis on applications in civil & environmental engineering. New York: Wiley; 2007.
- Smith GN. Probability and statistics in civil engineering. London: Collins Professional and Technical Books; 1986.
- Khosravikia F, Prakhov V, Potter A, Clayton P, Williamson E. Risk-based assessment of Texas bridges to natural and induced seismic hazards, Duluth, MN: ASCE Congress on Technical Advancement; 2017. p. 10–21. <https://doi.org/10.1061/9780784481028.002>. doi:<https://doi.org/10.1061/9780784481028.002>.
- Bommer JJ, Dost B, Edwards B, Stafford PJ, Van Elk J, Doornhof D, et al. Developing an application-specific ground-motion model for induced seismicity. *Bull Seismol Soc Am* 2016;106:158–73. <https://doi.org/10.1785/0120150184>.
- Khosravikia F, Zeinali Y, Nagy Z, Clayton P, Rathje E. Neural network-based equations for predicting PGA and PGV in Texas, Oklahoma, and Kansas, Geotechnical Earthquake Engineering and Soil Dynamics V, Austin, TX, USA; 2018. doi: <https://doi.org/10.1061/9780784481462.052>.
- Khosravikia F, Clayton P, Nagy Z. Artificial neural network based framework for developing ground motion models for natural and induced earthquakes in Texas, Oklahoma, and Kansas. *Seismol Res Lett* 2018;90(2A):604–13.
- Zalachoris G, Rathje EM. Ground motion model for small-to-moderate earthquakes in Texas, Oklahoma, and Kansas. *Earthquake Spectra* 2019;35:1–20.
- Ellsworth WL. Injection-induced earthquakes. *Science* 2013;341:1225942.
- Frohlich C, Ellsworth W, Brown WA, Brunt M, Luetgert J, MacDonald T, et al. The 17 May 2012 M4. 8 earthquake near Timpson, East Texas: An event possibly triggered by fluid injection. *J Geophys Res Solid Earth* 2014;119:581–93.
- Barbour AJ, Norbeck JH, Rubinstein JL. The effects of varying injection rates in Osage County, Oklahoma, on the 2016 M w 5.8 Pawnee earthquake. *Seismol Res Lett* 2017;88:1040–53.
- Sullivan I, Nielson BG. Sensitivity analysis of seismic fragility curves for skewed multi-span simply supported steel girder bridges. Structures congress 2010: 19th analysis and computation specialty conference. 2010. p. 226–37.
- FHWA. Recording and coding guide for the structure inventory and appraisal of the nation's bridges. Vol. FHWA-PD-96-001. Office of Engineering Bridge Division, Federal Highway Administration, McLean, VA.; 1995.
- Huntington DE, Lyrintzis CS. Improvements to and limitations of Latin hypercube sampling. *Probab Eng Mech* 1998;13:245–53.
- Nielson BG. Analytical fragility curves for highway bridges in moderate seismic zones. Doctoral dissertation, Georgia Institute of Technology; 2005.
- McKenna F, Fenves GL, Scott MH, et al. Open system for earthquake engineering simulation. Berkeley, CA: University of California; 2000.
- Nielson BG, DesRoches R. Analytical seismic fragility curves for typical bridges in the central and southeastern United States. *Earthquake Spectra* 2007;23:615–33.
- Filipov ET, Fahnstock LA, Steelman JS, Hajjar JF, LaFave JM, Foutch DA. Evaluation of quasi-isolated seismic bridge behavior using nonlinear bearing models. *Eng Struct* 2013;49:168–81.
- ACI. Code requirements for seismic evaluation and retrofit of existing concrete buildings. American Concrete Institute, Committee 369; 2016.
- ASCE. Seismic evaluation and retrofit of existing buildings. Reston, VA: ASCE/SEI 41-17; 2017.
- Ghannoum W, Sivaramakrishnan B. ACI 369 rectangular column database. Data set. Data set. < <http://www.nees.org/resources/3659> >; 2012. doi:<http://www.nees.org/resources/3659>.
- Ghannoum W, Sivaramakrishnan B. ACI 369 circular column database. Dataset. < <http://www.nees.org/resources/3658> >; 2012.
- Mander J, Kim D, Chen S, Premus G. Response of steel bridge bearings to the reversed cyclic loading. NCEER 96-0014, Buffalo, NY; 1996.
- Pan Y. Seismic fragility and risk management of highway bridges in New York State. Doctoral dissertation, City University of New York; 2007.
- Nielson BG. Analytical fragility curves for highway bridges in moderate seismic zones. *Environ Eng* 2005;400.